

# Evaluation of relationships between results of electrocardiography and echocardiography in 341 chimpanzees (*Pan troglodytes*)

Aimee L. Drane BSc

Rebeca Atencia PhD

Stephen-Mark Cooper PhD

Yedra Feltrer DVM

Thalita Calvi DVM

Tai Strike DVM

Christopher Palmer BAdvSci

Sarah Simcox BSc

Pablo Rodriguez DVM

Carlos Sanchez DVM, MSc

Hester van Bolhuis DVM

Bruce Peck DVM

Jaclyn Eng DVM

Sophie Moittie DVM

Steve Unwin DVM

Glyn Howatson PhD

David Oxborough PhD

Mike R. Stemberge PhD

Rob E. Shave PhD

Received May 8, 2019.  
Accepted November 8, 2019.

From the School of Sport and Health Sciences, International Primate Heart Project, Cardiff Metropolitan University, Cardiff CF5 2YB, England (Drane, Cooper, Feltrer, Simcox, Unwin, Stemberge); Tchimpouna Chimpanzee Sanctuary, Jane Goodall Institute, Pointe Noire, Republic of Congo (Atencia); Chimfunshi Wildlife Orphanage Trust, Chingola 50100, Zambia (Calvi, Peck); Zoological Society of London, Veterinary Department, London Zoo, Regents Park, London NW1 4RY, England (Strike); Department of Biological Science, University of New South Wales, Sydney, NSW 2052, Australia (Palmer); Buin Zoo, Buin, Chile (Rodriguez); Veterinary Medical Center, Oregon Zoo, Portland, OR 97221 (Sanchez); Animal Advocacy and Protection Rescue Centre for Exotic Animals, Almere, Netherlands (van Bolhuis); International Animal Rescue, Ketapang, West Kalimantan, Indonesia (Eng); Tacugama Chimpanzee Sanctuary, Freetown, Sierra Leone (Moittie); Faculty of Health and Life Sciences, Northumbria University, Newcastle-upon-Tyne NE7 7XA, England (Howatson); Water Research Group, Unit for Environmental Sciences and Management, North-West University, Potchefstroom 2531, South Africa (Howatson); Faculty of Science, Liverpool John Moores University, Liverpool L3 5UA, England (Oxborough); and Department of Health and Exercise Sciences, Faculty of Health and Social Development, University of British Columbia, Okanagan Campus, Kelowna, BC V1V 1V7, Canada (Shave).

Address correspondence to Dr. Drane (adrane@cardiffmet.ac.uk).

## OBJECTIVE

To examine potential relationships between ECG characteristics and echocardiographic measures of cardiac structure in chimpanzees (*Pan troglodytes*).

## ANIMALS

341 chimpanzees (175 males and 166 females) from 5 sanctuaries and 2 zoological collections.

## PROCEDURES

Chimpanzees were anesthetized for routine health examinations between May 2011 and July 2017 as part of the International Primate Heart Project and, during the same anesthetic events, underwent 12-lead ECG and transthoracic echocardiographic assessments. Relationships between results for ECG and those for echocardiographic measures of atrial areas, left ventricular internal diameter in diastole (LVIDd), and mean left ventricular wall thicknesses (MLVWT) were assessed with correlational analysis, then multiple linear regression analyses were used to create hierarchical models to predict cardiac structure from ECG findings.

## RESULTS

Findings indicated correlations ( $r = -0.231$  to  $0.310$ ) between results for ECG variables and echocardiographic measures. The duration and amplitude of P waves in lead II had the strongest correlations with atrial areas. The Sokolow-Lyon criteria, QRS-complex duration, and R-wave amplitude in leads  $V_6$  and II had the strongest correlations with MLVWT, whereas the Sokolow-Lyon criteria, QRS-complex duration, and S-wave amplitude in leads  $V_2$  and  $V_1$  had the strongest correlations with LVIDd. However, the ECG predictive models that were generated only accounted for 17%, 7%, 11%, and 8% of the variance in the right atrial end-systolic area, left atrial end-systolic area, MLVWT, and LVIDd, respectively.

## CONCLUSIONS AND CLINICAL RELEVANCE

Results indicated that relationships existed between ECG findings and cardiac morphology in the chimpanzees of the present study; however, further research is required to examine whether the predictive models generated can be modified to improve their clinical utility. (*Am J Vet Res* 2020;81:488–498)

## ABBREVIATIONS

BM	Body mass
DCM	Dilated cardiomyopathy
LAAS	Left atrial end-systolic area
LV	Left ventricle
LVH	Left ventricular hypertrophy
LVIDd	Left ventricular internal diameter in diastole
MLVWT	Mean left ventricular wall thickness
$R^2_{adj}$	Adjusted coefficient of determination
RAAS	Right atrial end-systolic area
SLV15	Sokolow-Lyon voltage sum of the S-wave amplitude in lead $V_1$ + the greatest R-wave amplitude in lead $V_5$
SLV25	Sokolow-Lyon voltage sum of the S-wave amplitude in lead $V_2$ + the greatest R-wave amplitude in lead $V_5$

Cardiovascular disease has been suggested as the leading cause of death in captive populations of chimpanzees (*Pan troglodytes*).<sup>1–4</sup> Specifically, conditions such as arterial hypertension,

congestive cardiac failure, and idiopathic myocardial fibrosis have been described.<sup>1,3,5-8</sup> In humans, specific patterns of cardiac remodeling (eg, atrial and ventricular dilatation and hypertrophy) are often the hallmark of cardiac disease (eg, hypertrophic cardiomyopathy, aortic stenosis, and congestive heart failure). Furthermore, adverse remodeling is related to an increased risk of cardiac events and poor prognosis in humans<sup>9,10</sup> and other species.<sup>11-14</sup> Importantly, however, cardiac remodeling in some conditions can be reversed with lifestyle adaptations and pharmacological agents, and such reversal is related to an improvement in overall prognosis.<sup>13-15</sup> Accordingly, the ability to detect cardiac remodeling is important for the diagnosis and ongoing treatment of cardiac disease.

Although cardiac imaging (echocardiography and MRI) is the optimal method for detecting adverse remodeling, this is not always possible, especially in species (eg, chimpanzees) being cared for in remote settings. Accordingly, the identification of other, more accessible diagnostic tools would be beneficial. In a number of species, the relationship between the ECG results and measures of cardiac structure has been used to develop diagnostic criteria that are potentially indicative of adverse remodeling.<sup>16-21</sup> However, this relationship has not been examined in chimpanzees; thus, the clinical utility of ECG in this critically endangered species is limited. Exploring whether specific ECG characteristics relate to cardiac morphology in chimpanzees is the first step in potentially developing useful diagnostic criteria. Therefore, the initial aim of the study presented here was to use a large heterogeneous sample of chimpanzees to examine whether relationships existed between results for ECG variables and results for echocardiographic measures of atrial areas, LV wall thicknesses, and chamber dimension, independent of body size. If relationships between results for ECG and echocardiography were detected, then the secondary aim was to develop initial ECG prediction equations that might provide veterinary teams an initial screening tool to assess cardiac structure in chimpanzees.

## Materials and Methods

### Animals

Chimpanzees eligible for the study were those that underwent complete cardiac examinations during routine health assessments between May 2011 and July 2017 as part of the International Primate Heart Project and that were housed at any of 3 sanctuaries for chimpanzees in Africa (the Tchimpounga Chimpanzee Rehabilitation Centre, Congo; Chimfunshi Wildlife Orphanage Trust, Zambia; and Tacugama Chimpanzee Sanctuary, Sierra Leone), 2 zoological parks in England (Chester Zoo and Zoological Society of London Whipsnade Zoo), or 2 sanctuaries for chimpanzees in Europe (Welsh Ape and Monkey Sanctuary, England, and Animal Advocacy and Protec-

tion Rescue Centre for Exotic Animals, Netherlands). Animals were categorized according to whether they were ex-research chimpanzees, zoo-housed chimpanzees, or African-sanctuary chimpanzees. Data for males versus females were also considered.

### Health and cardiac assessments

All cardiac examinations were completed during preplanned health assessments, and as such, the cohort included was a convenience sample. All health assessments were conducted at the housing facilities and by experienced veterinarians as previously described.<sup>22,23</sup> Briefly, once a chimpanzee was anesthetized and unresponsive to external stimuli, the animal was weighed, then transported to an assessment area, where a full health assessment was completed. Each health assessment included a thorough physical examination, blood sampling, morphometric measurements, and cardiac assessment with 12-lead ECG and transthoracic echocardiography. Body weight was used as a surrogate for BM.

**Anesthesia**—Chimpanzees were anesthetized with 1 of 5 protocols: a combination of medetomidine (0.03 to 0.05 mg/kg) and ketamine hydrochloride (3 to 5 mg/kg) administered IM by hand injection (MK), tiletamine-zolazepam (10 mg/kg) administered by remote dart injection (TZ), a combination of tiletamine-zolazepam (2 mg/kg) and medetomidine (0.03 mg/kg) administered by remote dart injection (TZM), a combination of tiletamine-zolazepam (2 mg/kg) and ketamine (5 mg/kg) administered by remote dart injection (TZK), or a combination of tiletamine-zolazepam (2.5 to 3 mg/kg) and detomidine (40 to 50 µg/kg) administered by remote dart injection (TZD). Following completion of health assessments on animals anesthetized with medetomidine or detomidine, atipamezole (0.25 mg/kg, IM) was administered to reverse anesthesia.

**ECGs**—Chimpanzees were positioned in supine recumbency for the 12-lead ECG (with leads I, II, III, aVL, aVF, aVR, V<sub>1</sub>, V<sub>2</sub>, V<sub>3</sub>, V<sub>4</sub>, V<sub>5</sub>, and V<sub>6</sub>). Following skin preparation with an alcohol wipe, ECG lead electrodes were placed as previously described<sup>24</sup> and in line with human protocols.<sup>25</sup> The ECGs were recorded with commercially available machines<sup>a,b</sup> set at a paper speed of 25 mm/s and a gain of 10 mm/mV and were later analyzed by an experienced cardiac physiologist (ALD). Findings from previous studies (eg, in humans,<sup>16,18,26-38,c</sup> dogs,<sup>39,40</sup> cats,<sup>20,21,41</sup> and rats<sup>42</sup>) that examined relationships between ECG results and cardiac structure informed our selection of the specific ECG characteristics that we examined in relation to echocardiographic measures of cardiac structure in chimpanzees. Mean ± SD electrical axes of P waves, QRS complexes, and T waves were quantified. Durations of P waves, QRS complexes, R-R intervals, and QT intervals were measured in limb leads and precordial leads. In addition, because the QT interval is dependent on the heart rate, the Bazett formula<sup>43</sup> was used to calculate a QT interval corrected for heart

rate. Voltage amplitudes of P, R, S, and Q waves and positive and negative deflections of ST segments and T waves were also measured in limb leads and precordial leads. In addition, the Sokolow-Lyon criteria values were calculated<sup>44</sup> as potential indicators of LVH,<sup>24</sup> with the sum of the voltage amplitudes of the S wave in V<sub>1</sub> and the R wave in V<sub>5</sub> for the SLV15, and with the sum of the voltage amplitudes of the S wave in V<sub>2</sub> and the R wave in V<sub>5</sub> for the SLV25.

**Echocardiography**—After undergoing ECG, chimpanzees were positioned in left lateral recumbency for comprehensive transthoracic echocardiography, which was completed with a commercially available ultrasound machine<sup>d</sup> and probes<sup>e,f</sup> as previously described<sup>23</sup> and in line with human guidelines.<sup>25,45–47</sup> To minimize measurement variability inherent with composite echocardiographic measures and to not make any assumptions regarding cardiac geometry in chimpanzees, we chose to use measures of areas and dimensions, instead of measures of volume or mass. Atrial size was determined as the LAAS and RAAS measured in the apical 4-chamber view.<sup>45</sup> The MLVWT was calculated as the mean of the LV septal and posterior wall thicknesses measured in the parasternal long-axis view.<sup>45</sup> The LVIDD was adopted as a surrogate of LV size and was measured in the parasternal long-axis view.<sup>45</sup> All echocardiographic images were analyzed with dedicated software<sup>g</sup> by an experienced echocardiographer (ALD), and all measurements were made in accordance with recommended guidelines.<sup>25,45,46</sup>

## Scaling of echocardiographic variables

Because the aim was to assess whether relationships exist between ECG results and echocardiographic measures of cardiac size and wall thicknesses, and because there is a strong relationship between cardiac size and body size, the echocardiographic measures were allometrically scaled to BM, for which body weight was used as a surrogate, to remove the influence of body size on the correlational and hierarchical analysis.<sup>48,49</sup> Body mass-scaling exponents were generated for each of the echocardiographic measures. These exponents were derived from the slope of the linear log-log plot of BM with each of the echocardiographic measures as recommended<sup>50</sup> Following scaling, BM independence was assessed with Pearson correlation coefficient analysis between BM and each of the scaled echocardiographic variables. Results for the scaled echocardiographic variables were then correlated with the results for the ECG variables and entered into hierarchical regression.

## Statistical analysis

To explore potential relationships between results for echocardiography and results for ECG, Pearson correlation coefficient (*r*) analysis was performed. The  $\alpha$  was set at 0.05, and the strength of the correlations were classified as negligible (*r* = 0.00 to 0.30), low (*r* = 0.30 to 0.50), or moderate (*r* = 0.50 to 0.70).<sup>50</sup> When a significant correlation was identified,

the specific ECG variables were entered into a regression model as independent variables in a hierarchical format (ie, highest to lowest  $R^2_{\text{adj}}$ ). If an independent variable did not substantially improve the  $R^2_{\text{adj}}$  value (determined from the statistical significance of the summary *F* ratio), it was removed from the model. Selection of the optimal model was made with reference to the highest  $R^2_{\text{adj}}$  value with the lowest SE of the estimate. Linearity and homoscedasticity were confirmed through observation of scatterplots from the relevant results. The independence of residuals was assessed with the Durbin-Watson statistic, and multicollinearity was assessed with tolerance values. Outliers were examined with Cook distance and leverage points for influence over the model, and individual studentized residuals with Cook distance > 1 and leverage points > 0.2 were deleted.<sup>51</sup>

To more fully explore relationships between results for ECG and results for echocardiography, a diverse sample of chimpanzees was purposely included. To better characterize the overall sample population, 1-way ANCOVA with Bonferroni post hoc analysis was used to examine differences in results by age, BM, and crown-to-rump length for the 3 categories of animals (ie, ex-research chimpanzees, zoo-housed chimpanzees, and African-sanctuary chimpanzees). However, we purposely chose not to include the captive environment variable in our models because our primary aim was to explore the potential for ECG variables to be used as predictors of cardiac structure, not to examine the influence of environment on cardiac phenotype. All statistical analyses were conducted with dedicated software.<sup>h</sup>

**Presentation of predictive models**—Predictive models were presented in the form:

$$Y = a + b_1X_1 + b_2X_2 + b_3X_3 + \dots + b_kX_k + e$$

where *a* is the intercept on the y-axis of an X-Y scatterplot, *b* is the  $\beta$  component (regression coefficient for a given independent variable), and *e* is the SE of the estimate, which estimated the proportion of the variance in the *Y* variable (dependent variable) unexplained by the model. Each of the regression coefficients ( $\beta$  components) estimated the amount of change that occurred in the dependent variable for a 1-unit change in the related independent variable, with the effect of all other independent variables in the equation controlled. Each model had a different level of *e* in the prediction of the echocardiographic variable. The model output  $\pm (e \times 1.96)$  provided the 95% CI of prediction for each model.

## Results

### Animals

Between May 2011 and July 2017, the International Primate Heart Project completed cardiac examinations of 341 chimpanzees (175 males and 166 females) during routine health assessments (**Table 1**). Of these 341 chimpanzees, 34 were ex-research chimpanzees (18

**Table 1**—Summary demographic and morphometric data for 341 chimpanzees (*Pan troglodytes*), stratified by population category (African-sanctuary chimpanzees, ex-research chimpanzees, or zoo-housed chimpanzees) and sex (male or female), that underwent general anesthesia for routine health examinations, 12-lead ECG, and echocardiography between May 2011 and July 2017 as part of the International Primate Heart Project.

Variable	African-sanctuary chimpanzees				Ex-research chimpanzees				Zoo-housed chimpanzees				All chimpanzees	
	Males (n = 148)		Females (n = 139)		Males (n = 18)		Females (n = 16)		Males (n = 9)		Females (n = 11)		(n = 341)	
	Mean ± SD	Range	Mean ± SD	Range	Mean ± SD	Range	Mean ± SD	Range	Mean ± SD	Range	Mean ± SD	Range	Mean ± SD	Range
Age (y)	14 ± 8	1–37	15 ± 7	1–38	32 ± 9*	16–55	32 ± 9*	21–52	31 ± 15†	9–51	29 ± 9*	17–42	17 ± 10	1–5
BM (kg)	42 ± 16	4–75	37 ± 11	4–65	56 ± 9*	43–73	57 ± 5*	49–64	61 ± 8*	42–70	59 ± 10*	45–81	42 ± 15	4–81
Crown-to-rump length (cm)	64 ± 11	28–89	63 ± 9	30–86	77 ± 5*	71–85	76 ± 6*	65–87	81 ± 3*	76–84	68 ± 5	63–79	66 ± 10	28–89

\*Results differed significantly ( $P < 0.001$ ) from those of African-sanctuary chimpanzees. †Results differed significantly ( $P < 0.05$ ) from those of African-sanctuary chimpanzees.

**Table 2**—Summary of the key results from 12-lead ECG (with leads I, II, III, aVL, aVF, aVR, V<sub>1</sub>, V<sub>2</sub>, V<sub>3</sub>, V<sub>4</sub>, V<sub>5</sub>, and V<sub>6</sub>) assessments of the chimpanzees described in Table 1.

Variable	Mean ± SD	Range
Heart rate (beats/min)	70 ± 31	41 to 101
Waveform mean electrical axes (°)		
P	57.0 ± 27.9	–49 to 133
QRS	52.7 ± 26.7	–90 to 94
T	40.7 ± 26.5	–126 to 90
Waveform durations (ms)		
R-R interval	877.1 ± 397.6	87 to 1,472
P	97.1 ± 42.6	58 to 200
QRS	83.5 ± 38.2	52 to 230
QT	387.1 ± 170.8	280 to 544
QTc	408.3 ± 180.3	39 to 534
Waveform amplitudes (mV)		
P <sub>II</sub>	0.10 ± 0.10	–0.07 to 0.25
R <sub>II</sub>	1.10 ± 0.50	0.03 to 2.96
S <sub>II</sub>	–0.10 ± 0.10	–0.58 to 0.40
ST <sub>II</sub>	0.10 ± 0.50	–0.11 to 1.0
T POS <sub>II</sub>	0.20 ± 0.10	–0.35 to 0.72
T NEG <sub>II</sub>	0.0 ± 0.0	–0.16 to 0.18
T POS <sub>III</sub>	0.1 ± 0.1	–0.17 to 0.41
T NEG <sub>III</sub>	0.0 ± 0.0	–0.15 to 0.42
R aVL	0.24 ± 0.14	0.01 to 1.07
R aVF	0.94 ± 0.52	0.03 to 2.6
T POS aVF	0.15 ± 0.13	–0.32 to 0.62
T NEG aVF	0.02 ± 0.03	–0.16 to 0.29
S V <sub>1</sub>	–1.10 ± 0.61	–2.9 to 1.1
S V <sub>2</sub>	–1.09 ± 0.61	–3 to 1.2
S V <sub>3</sub>	–0.76 ± 0.46	–3.59 to 0.3
R V <sub>5</sub>	1.73 ± 0.78	0.03 to 4.61
ST V <sub>5</sub>	0.10 ± 0.06	–0.04 to 0.31
T POS V <sub>5</sub>	0.32 ± 0.24	–0.26 to 1.41
T NEG V <sub>5</sub>	0.02 ± 0.02	–0.06 to 0.13
R V <sub>6</sub>	0.97 ± 0.40	0.03 to 2.7
ST V <sub>6</sub>	0.04 ± 0.04	–0.47 to 0.3
T POS V <sub>6</sub>	0.19 ± 0.11	–0.25 to 0.6
T NEG V <sub>6</sub>	0.01 ± 0.01	–0.06 to 0.17
Sokolow-Lyon criteria (mV)		
SLV15	3.03 ± 1.10	0.95 to 6.81
SLV25	3.01 ± 1.10	0.76 to 7.1

P = P wave. QRS = QRS complex. QT = QT interval. QTc = QT interval corrected (with the Bazett formula<sup>43</sup>) for heart rate. R = R wave. S = S wave. ST = ST segment. T = T wave. T NEG = Negative deflection of the T wave. T POS = Positive deflection of the T wave.

males and 16 females), 20 were zoo-housed chimpanzees (9 males and 11 females), and 287 were African-sanctuary chimpanzees (148 males and 139 females). The sample heterogeneity, with wide ranges in ages (range, 1 to 55 years), BM (range, 4 to 81 kg), and crown-to-rump lengths (range, 28 to 89 cm), made the chimpanzees of the study an ideal cohort to initially explore the relationships of interest. Mean ± SD BM was greater in zoo-housed chimpanzees (61 ± 8 kg for males and 59 ± 10 kg for females) and ex-research chimpanzees (56 ± 9 kg for males and 57 ± 5 kg for females) than in African-sanctuary chimpanzees (42 ± 16 kg for males and 37 ± 11 kg for females). Subjectively, zoo-housed and ex-research chimpanzees also appeared to have had greater subcutaneous fat than did African-sanctuary chimpanzees.

## Cardiac variables

For examinations, chimpanzees underwent general anesthesia achieved with 1 of 5 protocols: MK (n = 184; 92 males and 92 females), TZ (29; 14 males and 15 females), TZM (67; 40 males and 27 females), TZK (27; 11 males and 16 females), and TZD (34; 18 males and 16 females). Electrocardiographic and echocardiographic results were compiled (**Tables 2 and 3**). Overall, there were wide ranges in results for ECG and echocardiography. Mean ± SD heart rate, P-wave duration and amplitude, and QRS-complex duration were 70 ± 31 beats/min, 97.1 ± 42.6 milliseconds, 0.1 ± 0.1 mV, and 83.5 ± 38.2 milliseconds, respectively. Mean ± SD LAAS, RAAS, MLVWT, and LVIDd were 16 ± 5 cm<sup>2</sup>, 9 ± 3 cm<sup>2</sup>, 0.70 ± 0.20 cm, and 4.2 ± 0.7 cm, respectively. Although most (314/341 [92.1%]) chimpanzees did not have overt cardiac remodeling, echocardiography revealed abnormal cardiac morphology, including suspected LVH (n = 15), dilated LV (6), and dilated atria (9). Of note, 1 chimpanzee had extreme LVH (MLVWT, 1.62 cm; reference range, 0.55 to 1.1 cm<sup>23</sup>) on echocardiography and an SLV25 of 5.5 mV (reference range, 1.7 to 5.8 mV<sup>24</sup>).

## Echocardiographic variables scaled for BM

Body mass-scaling exponents were derived from the slope of the linear log-log plot of BM with each of the echocardiographic variables. Resultant expo-

**Table 3**—Summary echocardiographic results for LAAS, RAAS, MLVWT, and LVIDd in the chimpanzees described in Table 1, stratified by population category and sex.

Variable	African-sanctuary chimpanzees				Ex-research chimpanzees				Zoo-housed chimpanzees				All chimpanzees	
	Males (n = 148)		Females (n = 139)		Males (n = 18)		Females (n = 16)		Males (n = 9)		Females (n = 11)		(n = 341)	
	Mean $\pm$ SD	Range	Mean $\pm$ SD	Range	Mean $\pm$ SD	Range	Mean $\pm$ SD	Range	Mean $\pm$ SD	Range	Mean $\pm$ SD	Range	Mean $\pm$ SD	Range
LAAS (cm <sup>2</sup> )	16 $\pm$ 5	4–28	15 $\pm$ 3	4–23	23 $\pm$ 3	19–30	20 $\pm$ 3	16–24	19 $\pm$ 6	14–32	19 $\pm$ 6	14–32	16 $\pm$ 5	4–32
RAAS (cm <sup>2</sup> )	9 $\pm$ 3	3–19	8 $\pm$ 2	3–14	14 $\pm$ 3	10–22	11 $\pm$ 1	8–13	10 $\pm$ 3	6–18	12 $\pm$ 5	6–25	9 $\pm$ 3	2–25
MLVWT (cm)	0.71 $\pm$ 0.19	0.30–1.62	0.60 $\pm$ 0.12	0.30–0.90	1.00 $\pm$ 0.19	0.60–1.40	0.89 $\pm$ 0.24	0.40–1.30	0.92 $\pm$ 0.24	0.60–1.35	0.79 $\pm$ 0.12	0.65–1.00	0.70 $\pm$ 0.20	0.30–1.62
LVIDd (cm)	4.3 $\pm$ 0.8	2.1–7.0	3.9 $\pm$ 0.5	1.8–4.9	4.9 $\pm$ 0.4	4.3–5.9	4.3 $\pm$ 0.4	3.4–4.8	4.7 $\pm$ 0.8	3.8–6.1	4.6 $\pm$ 0.5	4.0–5.6	4.2 $\pm$ 0.7	1.8–7.0

**Table 4**—Results of Pearson correlation coefficient (*r*) analysis between results for echocardiographic variables (LAAS, RAAS, MLVWT, and LVIDd) scaled for BM and results for ECG variables described in Table 2 for the chimpanzees described in Table 1.

ECG variable	BM-scaled echocardiographic variables			
	LAAS ( <i>r</i> )	RAAS ( <i>r</i> )	MLVWT ( <i>r</i> )	LVID ( <i>r</i> )
Waveform mean electrical axes				
P	0.142*	0.830	—	—
QRS	0.023	−0.013	0.190	0.108*
T	−0.048	0.953	−0.088	0.074
Waveform durations				
P	0.235†	0.176†	—	—
QRS	—	—	0.229†	0.243†
QT	0.050	0.039	0.016	0.205†
QTc	0.093	−0.049	0.066	−0.089
Waveform amplitudes				
P <sub>II</sub>	0.201†	0.176†	—	—
R <sub>II</sub>	—	—	0.205†	0.090
S <sub>II</sub>	—	—	—	—
ST <sub>II</sub>	—	—	0.050	−0.009
T POS <sub>II</sub>	—	—	−0.097	−0.099
T NEG <sub>II</sub>	—	—	0.051	−0.028
T POS <sub>III</sub>	—	—	−0.121*	−0.064
T NEG <sub>III</sub>	—	—	0.028	−0.003
R aVL	—	—	0.050	0.115*
R aVF	—	—	0.198†	0.137†
T POS aVF	—	—	−0.095	−0.024
T NEG aVF	—	—	0.051	−0.005
S V <sub>1</sub>	—	—	−0.217*	−0.223†
S V <sub>2</sub>	—	—	−0.231*	−0.231†
S V <sub>3</sub>	—	—	−0.233*	−0.231†
R V <sub>5</sub>	—	—	0.246†	0.175*
ST V <sub>5</sub>	—	—	0.109*	−0.020
T POS V <sub>5</sub>	—	—	0.090	−0.043
T NEG V <sub>5</sub>	—	—	0.080	−0.058
R V <sub>6</sub>	—	—	0.229†	0.134†
ST V <sub>6</sub>	—	—	0.060	−0.055
T POS V <sub>6</sub>	—	—	−0.098	−0.107
T NEG V <sub>6</sub>	—	—	−0.020	−0.072
Sokolow-Lyon criteria (mV)				
SLV15	—	—	0.308†	0.261†
SLV25	—	—	0.310†	0.266†

\**P* < 0.05. †*P* < 0.001.

— = Not assessed.

See Table 2 for remainder of the key.

nents were LAAS/BM<sup>0.612</sup>, RAAS/BM<sup>0.591</sup>, MLVWT/BM<sup>0.451</sup>, and LVIDd/BM<sup>0.3224</sup>. Independence of BM was then confirmed with the findings of nonsignificant

correlations (Pearson correlation coefficient analysis) between each of the scaled echocardiographic variables and BM.

## Correlational analysis

Results of Pearson correlations coefficient (*r*) analysis between findings for ECG variables and echocardiographic variables (ie, RAAS, LAAS, MLVWT, and LVIDd) scaled for BM were compiled (Table 4). Results for P-wave duration and amplitude in lead II significantly (*P* < 0.05) correlated with results for LAAS and RAAS scaled for BM. In addition, results for several ECG variables significantly (*P* < 0.05) correlated with MLVWT scaled for BM, with the strongest relationships detected between it and SLV15 (*r* = 0.308), SLV25 (*r* = 0.310), QRS-complex duration (*r* = 0.229), and R-wave amplitude in leads V<sub>5</sub>, V<sub>6</sub>, and II (*r* = 0.246, *r* = 0.229, and *r* = 0.205, respectively). Similarly, significant (*P* < 0.05) correlations were also identified between results for LVIDd scaled for BM and results for ECG variables, including SLV15 (*r* = 0.216), SLV25 (*r* = 0.226), QRS-complex duration (*r* = 0.243), QT interval (*r* = 0.205), and S-wave amplitude in leads V<sub>1</sub>, V<sub>2</sub>, and V<sub>3</sub> (*r* = −0.223, *r* = −0.231, and *r* = −0.231, respectively).

## Predictive models

Through hierarchical regression, predictive models for RAAS, LAAS, MLVWT, and LVIDd scaled for BM were developed. These predictive models accounted for 17%, 7%, 11%, and 8% of the variance in RAAS, LAAS, MLVWT, and LVIDd, respectively (Figure 1; Table 5). Because a number of different anesthetic protocols were used, the influence of anesthetic protocols on the models was explored. However, inclusion of anesthetic protocols into the models did not meaningfully improve the *R*<sup>2</sup><sub>adj</sub>; thus, anesthetic protocols were not included in the final models. There was no evidence of multicollinearity, as assessed by tolerance values, and there were no individual studentized deleted residuals with Cook distance > 1 and leverage points > 0.2 in any of the models.

## Discussion

The initial aim of the present study was to examine whether relationships exist between the ECG and echocardiographic measures of RAAS, LAAS, MLVWT, or LVIDd in chimpanzees, independent of body size. The second aim was to examine whether ECG models could be constructed that predict cardi-

**Table 5**—Results of hierarchical regression analysis to generate ECG predictive models for RAAS, LAAS, MLVWT, and LVIDd scaled to BM in the chimpanzees described in Table 1.

BM-scaled echocardiographic variables	$R^2_{adj}$	a	ECG variables	$\beta$	e	SE of $\beta$	95% CI of $\beta$
LAAS (cm <sup>2</sup> )	0.067	1.239	P-wave duration	0.004	0.27	0.001	0.001–0.006
			P-wave amplitude in lead II	0.874		0.338	0.209–1.539
RAAS (cm <sup>2</sup> )	0.173	1.303	P-wave duration	0.807	2.91	0.072	0.667–0.948
MLVWT (cm)	0.115	0.109	SLV25	0.006	0.02	0.001	0.003–0.008
			QRS-complex duration	0.001		0.001	0.001–0.002
LVIDd (cm)	0.080	1.087	SLV25	0.022	0.11	0.006	0.010–0.033
			QRS-complex duration	0.001		0.000	0.001–0.002

a = The intercept on the y-axis.  $\beta$  = Regression coefficient. e = SE of the estimate.

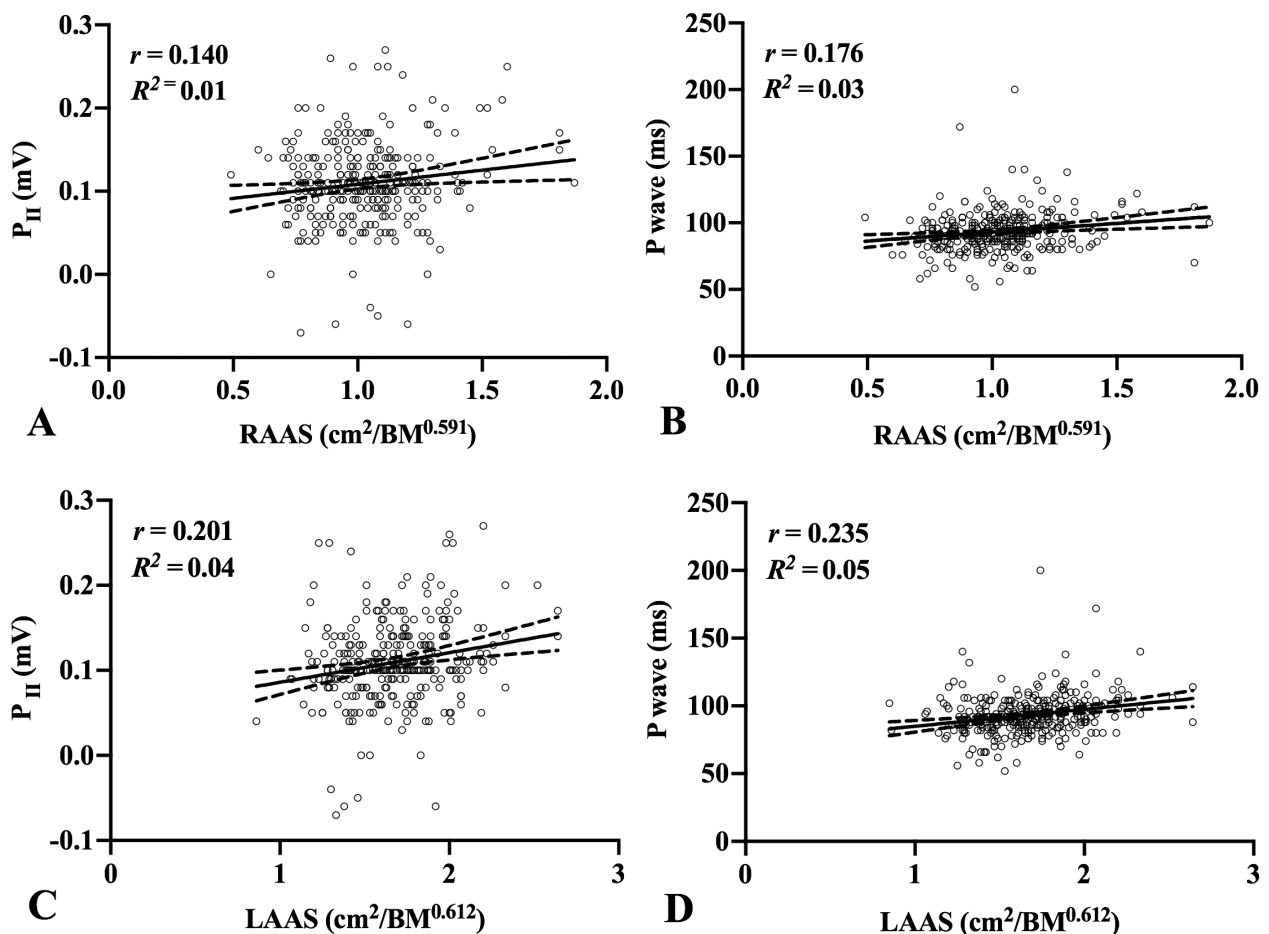
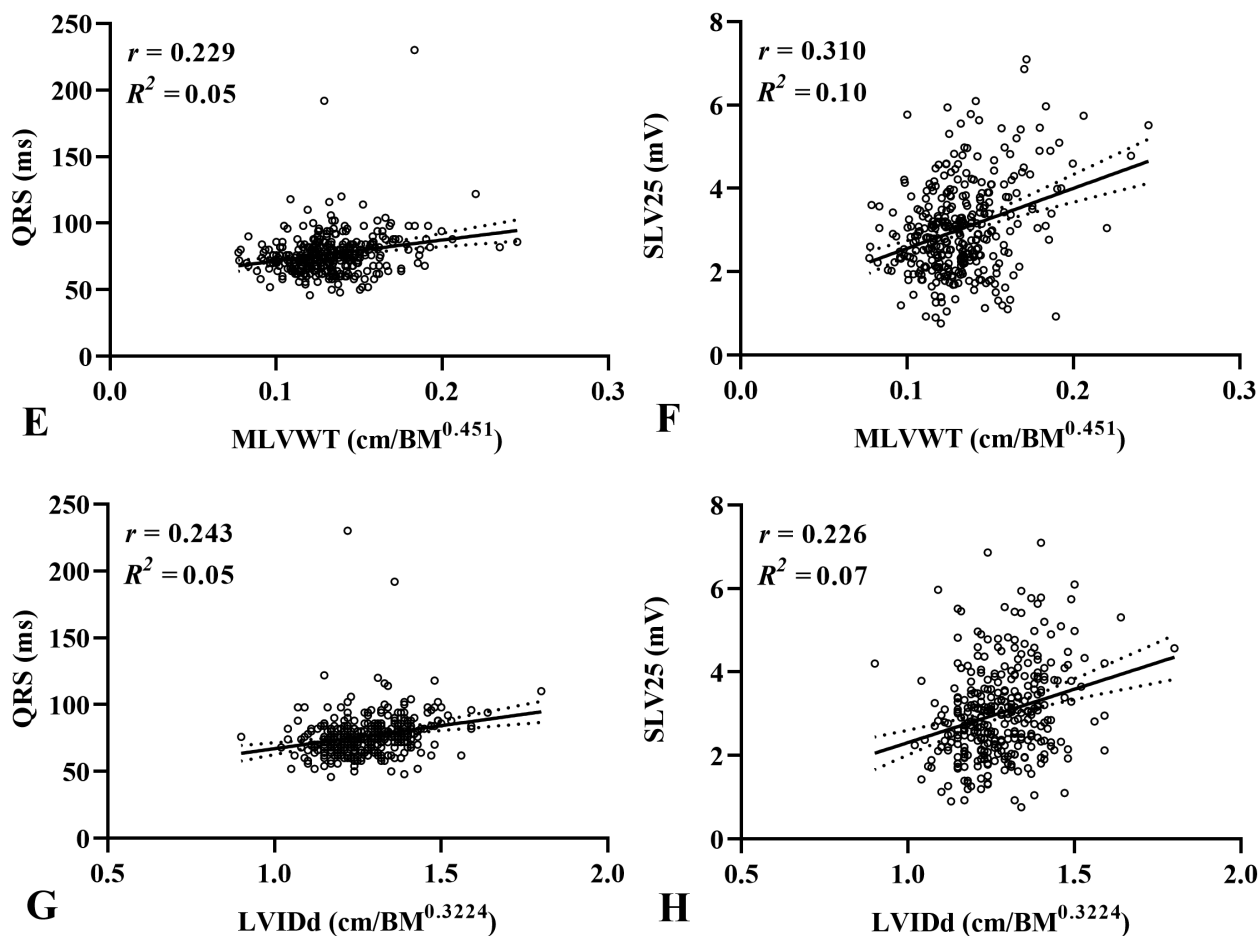


Figure 1 continues on the next page

ac structure and hence help the assessment of cardiac remodeling in chimpanzees. Our primary finding was that relationships, albeit weak, existed between results for multiple ECG variables and echocardiographic measures of cardiac structure in the chim-

panzees of the present study. The predictive models we generated accounted for 17%, 7%, 11%, and 8% of the variance in RAAS, LAAS, MLVWT, and LVIDd, respectively. Although our findings indicated that ECG results were related to cardiac structure in chimpan-



**Figure 1**—Scatterplots of results for ECG variables (P-wave amplitude [A and C] and duration [B and D] in lead II, QRS-complex duration [E and G], and SLV25 [F and H]) versus results for BM-scaled echocardiographic variables (RAAS [A and B], LAAS [C and D], MLVWT [E and F], and LVIDd [G and H]) for 341 chimpanzees (*Pan troglodytes*) that underwent general anesthesia for routine health examinations, 12-lead ECG, and echocardiography between May 2011 and July 2017 as part of the International Primate Heart Project. In each panel, the solid line represents the regression line, dotted lines represent the 95% CI limits of the regression line, and circles represent results for individual chimpanzees.

zees, it appeared that these ECG models cannot be used to accurately predict cardiac chamber sizes and wall thicknesses.

Our results indicated that P-wave duration and amplitude in lead II weakly correlated with end systolic atrial areas in chimpanzees. As the P wave reflects atrial depolarization, the finding that P-wave duration and amplitude were related to atrial areas in chimpanzees of the present study was unsurprising. It is rational that in animals with larger atria, the electrical propagation across the myocardium will take longer and have a greater amplitude. In humans<sup>16,21,34,52</sup> and cats,<sup>20,53</sup> P-wave amplitude, duration, axis, and morphology and PR interval have all been shown to be related to adverse atrial remodeling, with P-wave amplitude showing the strongest relationship.<sup>26,32,36</sup> Yet, in the chimpanzees of the present study, P-wave duration had a stronger relationship with atrial areas than did P-wave amplitude. Moreover, P-wave axis and morphology were not strongly related to atrial areas

in the present cohort. It has been reported<sup>24</sup> that chimpanzees have small P-wave amplitudes, compared with other ECG waveforms, and this could have explained the weaker correlation between P-wave amplitude and atrial areas in the present study. The cause of small P waves in chimpanzees is unknown but may reflect a different diastolic filling pattern in chimpanzees. Compared with humans, it appears that the atrial contribution to ventricular filling is relatively modest in chimpanzees.<sup>23</sup> As such, the atria might function more as a conduit rather than an active pump, and so the atrial myocardial mass and resulting P-wave amplitudes could be smaller in chimpanzees.

Findings from the present study suggested that the Sokolow-Lyon criteria; amplitudes of the R waves in leads II, aVF, V<sub>5</sub>, and V<sub>6</sub>; amplitudes of the S waves in leads V<sub>1</sub>, V<sub>2</sub>, and V<sub>3</sub>; QRS-complex duration; positive deflection of the T wave in lead III; and ST amplitude in lead V<sub>5</sub> are all related to MLVWT in chimpanzees. It is logical that electrical amplitude and

duration will increase as cardiac wall thicknesses increase, and our findings that the amplitudes of R and S waves weakly correlated with LV wall thicknesses in chimpanzees were similar to findings in humans,<sup>21,44,54</sup> cats,<sup>41</sup> and rats<sup>42</sup> in which voltage criteria are the most specific and sensitive for detecting LVH. However, there appeared to have been some chimpanzees in our study with thicker LV walls but without markedly large amplitudes of R and S waves. This finding could have indicated LV wall thickening from diffuse idiopathic myocardial fibrosis, as evidenced in other chimpanzee cohorts.<sup>6,7,55</sup> From our data, we did not know whether these thicker LV wall measurements reflected electrically active myocardium. For example, in humans with cardiac amyloidosis, despite LVH, QRS-complex amplitudes are low because the hypertrophy is caused by infiltration of electrically inactive tissue.<sup>56</sup> If some animals in our cohort did indeed have idiopathic fibrosis, this could have resulted in larger MLVWTs but not a concomitant increase in QRS-complex amplitudes.

In the chimpanzees of the present study, numerous ECG variables (including durations of QRS complexes and QT intervals; amplitudes of R waves in leads aVL, aVF, V<sub>5</sub>, and V<sub>6</sub>; and amplitudes of S waves in leads V1, V2, and V3) were related to LVIDd, and the Sokolow-Lyon criteria, QRS-complex duration, and R- and S-wave amplitudes had the strongest correlations. These findings were again similar to those in humans whereby amplitudes of R and S waves, duration of QRS complexes, and abnormalities of ST segments, T waves, and Q waves relate to increased ventricular chamber size.<sup>38,c</sup> Caution is needed when directly comparing findings of the present report with those in human medicine because ECG variables have been identified in humans with marked cardiac disease, such as DCM and LV dilatation related to valve disease.<sup>38,c</sup> Because the underlying causes of these conditions are different, the myocardial properties with each will result in specific disease-related ECG patterns. For example, histologic findings in DCM demonstrate a reduction in myocardial fiber mass with concomitant fiber elongation and hypertrophy, resulting in ECG findings of greater precordial QRS-complex amplitudes.<sup>57</sup> Yet, in end-stage DCM, amplitudes of QRS complexes are low because of replacement fibrosis.<sup>58</sup> Understanding the properties of the myocardium is therefore important for interpreting ECG alterations in various diseases. As noted previously, although we know that some chimpanzees in other populations have shown evidence of idiopathic myocardial fibrosis and appeared to have had a higher proportion of collagen in the myocardium, compared with that in humans,<sup>4</sup> the properties of the myocardium in the chimpanzees of the present study was not known. Accordingly, follow-up postmortem work would be required to ascertain any underlying cardiac disease and examine whether this may have impacted any of the relationships we assessed.

Although our findings indicated that a number of ECG variables correlated with echocardiographic measures of atrial and ventricular structure, the ECG predictive models, for the most part, only accounted for a small to modest amount of the variance (7% to 17%). Of the 4 predictive ECG models generated, the strongest was for predicting RAAS, which accounted for 17% of the variance. Putting this finding into context with existing human literature was challenging because most studies<sup>16,31,32,34–36,44,c</sup> explored the sensitivity and specificity of various ECG criteria in relation to a known diagnostic threshold or clinical end point, not relationships between results for ECG versus echocardiography. At present, diagnostic thresholds related to cardiac structure have yet to be established in chimpanzees; thus, it was not possible to explore the sensitivity or specificity of ECG characteristics in the present study. However, the low amount of variance accounted for by the models in the present study could have suggested that, as in humans,<sup>27</sup> ECG variables do not provide definitive information regarding cardiac chamber sizes and wall thicknesses in chimpanzees. In contrast, a study<sup>20</sup> of cats shows that ECG findings have some clinical utility in the diagnosis of LVH.

A major limitation of the present study was the lack of substantial cardiac diseases in our cohort. Historically, ECG criteria for detecting cardiac remodeling in humans<sup>16–19,21,38</sup> and animals (eg, cats,<sup>11,12,20</sup> dogs,<sup>38,39</sup> and rats<sup>42</sup>) have been based on research from large samples of abnormal and normal cardiac phenotypes. Although there was a range in cardiac morphology in chimpanzees of the present study, most animals did not have overt remodeling. Nonetheless, 1 chimpanzee had extreme LVH (MLVWT = 1.62 cm) identified with echocardiography and also had an SLV25 of 5.5 mV, which suggested that in chimpanzees with severe LVH, there may be a strong coupling of ECG results with the cardiac structural phenotype. Further work in a more diverse population of chimpanzees, including those with heart disease, would be required to confirm such a relationship. Beyond this, once clinical definitions of the clinically normal cardiac phenotype and specific cardiac diseases have been established in chimpanzees, it will be possible to explore the sensitivity and specificity of the ECG characteristics to identify adverse cardiac remodeling.

It is important to note that in humans and other animals, there is evidence that ECG results can be influenced by changes to body position, electrode placement, and body habitus.<sup>59–61</sup> In the present study, human guidelines were followed for patient positioning and electrode placement, and we recognized that these may not have been optimal for chimpanzees. Furthermore, body habitus influences durations and amplitudes of ECG waveforms in humans and other species.<sup>62–64</sup> In the present study, zoo-housed and ex-research chimpanzees had greater BM and subjectively more subcutaneous

fat than did the African-sanctuary chimpanzees. Although echocardiographic data were scaled to BM, this did not account for the influence of body fat percentage or, more specifically, the location of fat, which could have resulted in lower amplitudes for QRS complexes in the larger chimpanzees despite the presence of greater MLVWT in these animals. Therefore, as has been done in cats<sup>59</sup> and dogs,<sup>60</sup> future work should investigate the influence of ECG electrode placement and body habitus on the relationship between results for ECG versus cardiac morphology in chimpanzees.

In addition to the influence of body habitus on ECG voltages, body size is known to have a strong curvilinear relationship with cardiac size in a number of species.<sup>49,65</sup> Therefore, in the present study, cardiac chamber sizes and wall thickness were allometrically scaled to BM in an attempt to create body size-independent measures of cardiac structure. However, current scaling recommendations suggest lean BM and fat-free mass are likely the optimal body size scalar variables because they represent metabolically active tissue. The use of BM as a scalar variable, as in the present study, can be problematic, particularly if the proportions of muscle mass and adipose fat are not consistent across the sample studied.<sup>48,66</sup> It was possible that scaling to BM in our study may have resulted in an overcorrection of cardiac dimensions in overweight chimpanzees<sup>67</sup> from the zoo-housed and ex-research groups. Future work is needed to understand the relationships between body composition, cardiac size, and ECG results to generate an appropriate chimpanzee-specific body size scalar variable. If such an appropriate scalar variable can be generated, this in turn may improve the strength of the predictive models generated in the present study.

It is important that we acknowledge that all chimpanzees were anesthetized so that the routine health assessments could be completed safely, and we recognize that although the inclusion of anesthesia did not significantly improve the  $R^2_{adj}$  of the predictive models, anesthesia may have influenced our findings. Moreover, anesthetic agents could have contributed to some of the differences between ECG results of the present study, compared with other species, because, for instance, humans, cats, and dogs are not generally anesthetized for ECG. It has been suggested that general anesthesia influences cardiac rhythm and the durations of the ST-T segment, QT interval, and QT interval corrected for heart rate<sup>68-70</sup>; however, without knowing the direct impact of the various anesthetic protocols on the ECG results for the chimpanzees in the present study, it was impossible to speculate on this issue further.

Results of the present study were the first to indicate that relationships, albeit weak, existed between ECG findings and cardiac morphology in chimpanzees. However, the use of ECG to predict cardiac structure appears limited, and further work is needed

to improve predictive ECG models and their clinical utility in chimpanzees.

## Acknowledgments

The authors declare that there were no conflicts of interest.

## Footnotes

- a. CT800i interpretive ECG machine, Seca GmbH, Hamburg, Germany.
- b. Cardiovit MS-2015, Schiller Americas Inc, Doral, Fla.
- c. Houyuemei Z. The comparative analysis of ECG between ischaemic cardiomyopathy and dilated cardiomyopathy (abstr). *Heart* 2012;98(suppl 2):E167-E168.
- d. Vivid q, GE Vingmed Ultrasound, Horten, Norway.
- e. 6s pediatric cardiac ultrasound transducer, GE Vingmed Ultrasound, Horten, Norway.
- f. M4S adult cardiac ultrasound transducer, GE Vingmed Ultrasound, Horten, Norway.
- g. EchoPAC, PC version 112.1.0, GE Healthcare, Chicago, Ill.
- h. SPSS, version 24 for Windows, IBM Corp, Armonk, NY.

## References

1. Baldessari A, Snyder J, Ahrens J, et al. Fatal myocardial fibrosis in an aged chimpanzee (*Pan troglodytes*). *Pathobiol Aging Age Relat Dis* 2013;3:1-12.
2. Doane CJ, Lee DR, Sleeper MM. Electrocardiogram abnormalities in captive chimpanzees (*Pan troglodytes*). *Comp Med* 2006;56:512-518.
3. Seiler BM, Dick EJ Jr, Guardado-Mendoza R, et al. Spontaneous heart disease in the adult chimpanzee (*Pan troglodytes*). *J Med Primatol* 2009;38:51-58.
4. Varki N, Anderson D, Herndon JG, et al. Heart disease is common in humans and chimpanzees, but is caused by different pathological processes. *Evol Appl* 2009;2:101-112.
5. Ely JJ, Zavaskis T, Lammey ML, et al. Blood pressure reference intervals for healthy adult chimpanzees (*Pan troglodytes*). *J Med Primatol* 2011;40:171-180.
6. Hansen JF, Alford PL, Keeling ME. Diffuse myocardial fibrosis and congestive heart failure in an adult male chimpanzee. *Vet Pathol* 1984;21:529-531.
7. Lammey ML, Baskin GB, Gigliotti AP, et al. Interstitial myocardial fibrosis in a captive chimpanzee (*Pan troglodytes*) population. *Comp Med* 2008;58:389-394.
8. Ely JJ, Zavaskis T, Lammey ML. Hypertension increases with aging and obesity in chimpanzees (*Pan troglodytes*). *Zoo Biol* 2013;32:79-87.
9. Stewart MH, Lavie CJ, Shah S, et al. Prognostic implications of left ventricular hypertrophy. *Prog Cardiovasc Dis* 2018;61:446-455.
10. Vakili BA, Okin PM, Devereux RB. Prognostic implications of left ventricular hypertrophy. *Am Heart J* 2001;141:334-341.
11. Payne JR, Borgeat K, Brodbelt DC, et al. Risk factors associated with sudden death vs. congestive heart failure or arterial thromboembolism in cats with hypertrophic cardiomyopathy. *J Vet Cardiol* 2015;17:S318-S328.
12. Ferasin L. Feline myocardial disease: 1: classification, pathophysiology and clinical presentation. *J Feline Med Surg* 2009;11:3-13.
13. Pfeffer MA, Pfeffer JM. Ventricular enlargement and reduced survival after myocardial infarction. *Circulation* 1987;75:IV93-IV97.
14. Pfeffer MA, Pfeffer JM, Steinberg C, et al. Survival after an experimental myocardial infarction: beneficial effects of long-term therapy with captopril. *Circulation* 1985;72:406-412.
15. Fagard RH, Celis H, Thijs L, et al. Regression of left ventricular mass by antihypertensive treatment: a meta-analysis of randomized comparative studies. *Hypertension* 2009;54:1084-1091.
16. Hancock EW, Deal BJ, Mirvis DM, et al. Recommendations for the standardization and interpretation of the electrocardiogram: part V: electrocardiogram changes associated with

- cardiac chamber hypertrophy: a scientific statement from the American Heart Association Electrocardiography and Arrhythmias Committee, Council on Clinical Cardiology; the American College of Cardiology Foundation; and the Heart Rhythm Society: endorsed by the International Society for Computerized Electrocardiology. *J Am Coll Cardiol* 2009;53:992-1002.
17. Macfarlane PW, Van Oosterom A, Pahlm O, et al. *Comprehensive electrocardiology*. 2nd ed. London: Springer-Verlag London Ltd, 2010.
  18. Peguero JG, Lo Presti S, Perez J, et al. Electrocardiographic criteria for the diagnosis of left ventricular hypertrophy. *J Am Coll Cardiol* 2017;69:1694-1703.
  19. Aro AL, Chugh SS. Clinical diagnosis of electrical versus anatomic left ventricular hypertrophy: prognostic and therapeutic implications. *Circ Arrhythm Electrophysiol* 2016;9:e003629.
  20. Romito G, Guglielmini C, Mazzarella MO, et al. Diagnostic and prognostic utility of surface electrocardiography in cats with left ventricular hypertrophy. *J Vet Cardiol* 2018;20:364-375.
  21. Moise NS, Dietze AE, Mezza LE, et al. Echocardiography, electrocardiography, and radiography of cats with dilatation cardiomyopathy, hypertrophic cardiomyopathy, and hyperthyroidism. *Am J Vet Res* 1986;47:1476-1486.
  22. Atencia R, Stöhr EJ, Drane AL, et al. Heart rate and indirect blood pressure responses to four different field anesthetic protocols in wild-born captive chimpanzees (*Pan troglodytes*). *J Zoo Wildl Med* 2017;48:636-644.
  23. Drane AL, Atencia R, Cooper SM, et al. Cardiac structure and function characterized across age groups and between sexes in healthy wild-born captive chimpanzees (*Pan troglodytes*) living in sanctuaries. *Am J Vet Res* 2019;80:547-557.
  24. Atencia R, Revuelta L, Somauroo JD, et al. Electrocardiogram reference intervals for clinically normal wild-born chimpanzees (*Pan troglodytes*). *Am J Vet Res* 2015;76:688-693.
  25. Lang RM, Badano LP, Mor-Avi V, et al. Recommendations for cardiac chamber quantification by echocardiography in adults: an update from the American Society of Echocardiography and the European Association of Cardiovascular Imaging. *Eur Heart J Cardiovasc Imaging* 2015;16:233-270.
  26. Munuswamy K, Alpert MA, Martin RH, et al. Sensitivity and specificity of commonly used electrocardiographic criteria for left atrial enlargement determined by M-mode echocardiography. *Am J Cardiol* 1984;53:829-832.
  27. Pewsner D, Juni P, Egger M, et al. Accuracy of electrocardiography in diagnosis of left ventricular hypertrophy in arterial hypertension: systematic review. *BMJ* 2007;335:711.
  28. Romhilt DW, Estes EH Jr. A point-score system for the ECG diagnosis of left ventricular hypertrophy. *Am Heart J* 1968;75:752-758.
  29. Schack JA, Rosenman RH, Katz LN. The aV limb leads in the diagnosis of ventricular strain. *Am Heart J* 1950;40:696-705.
  30. Alpert MA, Munuswamy K. Electrocardiographic diagnosis of left atrial enlargement. *Arch Intern Med* 1989;149:1161-1165.
  31. Casale PN, Devereux RB, Kligfield P, et al. Electrocardiographic detection of left ventricular hypertrophy: development and prospective validation of improved criteria. *J Am Coll Cardiol* 1985;6:572-580.
  32. Chirife R, Feitosa GS, Frankl WS. Electrocardiographic detection of left atrial enlargement. Correlation of P wave with left atrial dimension by echocardiography. *Br Heart J* 1975;37:1281-1285.
  33. George A, Arumugham PS, Figueredo VM. aVR - the forgotten lead. *Exp Clin Cardiol* 2010;15:e36-e44.
  34. Goldberger E. *Unipolar lead electrocardiography*. 2nd ed. Philadelphia: Lea & Febiger, 1949.
  35. Gosse P, Jan E, Coulon P, et al. ECG detection of left ventricular hypertrophy: the simpler, the better? *J Hypertens* 2012;30:990-996.
  36. Hazen MS, Marwick TH, Underwood DA. Diagnostic accuracy of the resting electrocardiogram in detection and estimation of left atrial enlargement: an echocardiographic correlation in 551 patients. *Am Heart J* 1991;122:823-828.
  37. Kannel WB, Gordon T, Castelli WP, et al. Electrocardiographic left ventricular hypertrophy and risk of coronary heart disease. The Framingham study. *Ann Intern Med* 1970;72:813-822.
  38. Momiya Y, Mitamura H, Kimura M. ECG characteristics of dilated cardiomyopathy. *J Electrocardiol* 1994;27:323-328.
  39. Morales M, Ynaraja E, Montoya JA. Dilated cardiomyopathy in Presa Canario dogs: ECG findings. *J Vet Med A Physiol Pathol Clin Med* 2001;48:577-580.
  40. Vollmar AC, Aupperle H. Cardiac pathology in Irish Wolfhounds with heart disease. *J Vet Cardiol* 2016;18:57-70.
  41. Shechter JA, O'Connor KM, Friehling TD, et al. Electrophysiologic effects of left ventricular hypertrophy in the intact cat. *Am J Hypertens* 1989;2:81-85.
  42. Dunn FG, Pfeffer MA, Frohlich ED. ECG alterations with progressive left ventricular hypertrophy in spontaneous hypertension. *Clin Exp Hypertens* 1978;1:67-86.
  43. Bazett HC. An analysis of the time relations of electrocardiograms. *Heart* 1920;7:353-370.
  44. Sokolow M, Lyon TP. The ventricular complex in left ventricular hypertrophy as obtained by unipolar precordial and limb leads. *Am Heart J* 1949;37:161-186.
  45. Lang RM, Bierig M, Devereux RB, et al. Recommendations for chamber quantification: a report from the American Society of Echocardiography's Guidelines and Standards Committee and the Chamber Quantification Writing Group, developed in conjunction with the European Association of Echocardiography, a branch of the European Society of Cardiology. *J Am Soc Echocardiogr* 2005;18:1440-1463.
  46. Wharton GSAR, Brewerton J, Jones H, et al. *A standard echocardiogram: minimum dataset*. London: British Society of Echocardiography, 2012.
  47. Shave R, Oxborough D, Somauroo J, et al. Echocardiographic assessment of cardiac structure and function in great apes: a practical guide. *Int Zoo Yearb* 2014;48:218-233.
  48. Batterham AM, George KP, Whyte G, et al. Scaling cardiac structural data by body dimensions: a review of theory, practice, and problems. *Int J Sports Med* 1999;20:495-502.
  49. Dewey FE, Rosenthal D, Murphy DJ Jr, et al. Does size matter? Clinical applications of scaling cardiac size and function for body size. *Circulation* 2008;117:2279-2287.
  50. Hinkle DE, Wiersma W, Jurs SG. *Applied statistics for the behavioral sciences*. 2nd ed. Boston: Houghton Mifflin, 1988.
  51. Lewis-Beck MS. *Regression analysis*. London: SAGE Publications/Toppan Publishing, 1993.
  52. Tsao CW, Josephson ME, Hauser TH, et al. Accuracy of electrocardiographic criteria for atrial enlargement: validation with cardiovascular magnetic resonance. *J Cardiovasc Magn Reson* 2008;10:7.
  53. White AJM. End-stage hypertrophic cardiomyopathy in a cat. *Can Vet J* 2015;56:509-511.
  54. Okin PM, Jern S, Devereux RB, et al. Effect of obesity on electrocardiographic left ventricular hypertrophy in hypertensive patients: the losartan intervention for endpoint (LIFE) reduction in hypertension study. *Hypertension* 2000;35:13-18.
  55. Lammey ML, Lee DR, Ely JJ, et al. Sudden cardiac death in 13 captive chimpanzees (*Pan troglodytes*). *J Med Primatol* 2008;37:39-43.
  56. Cheng Z, Zhu K, Tian Z, et al. The findings of electrocardiography in patients with cardiac amyloidosis. *Ann Noninvasive Electrocardiol* 2013;18:157-162.
  57. Radu RI, Bold A, Pop OT, et al. Histological and immunohistochemical changes of the myocardium in dilated cardiomyopathy. *Rom J Morphol Embryol* 2012;53:269-275.
  58. Roberts WC, Siegel RJ, McManus BM. Idiopathic dilated cardiomyopathy: analysis of 152 necropsy patients. *Am J Cardiol* 1987;60:1340-1355.
  59. Harvey AM, Faena M, Darke PG, et al. Effect of body position on feline electrocardiographic recordings. *J Vet Intern Med* 2005;19:533-536.

60. Rishniw M, Porciello F, Erb HN, et al. Effect of body position on the 6-lead ECG of dogs. *J Vet Intern Med* 2002;16:69-73.
61. Rajaganesan R, Ludlam C, Francis D, et al. Accuracy in ECG lead placement among technicians, nurses, general physicians and cardiologists. *Int J Clin Pract* 2008;62:65-70.
62. VanHoose L, Sawers Y, Loganathan R, et al. Electrocardiographic changes with the onset of diabetes and the impact of aerobic exercise training in the Zucker Diabetic Fatty (ZDF) rat. *Cardiovasc Diabetol* 2010;9:56.
63. Mutiso SK, Rono DK, Bukachi F. Relationship between anthropometric measures and early electrocardiographic changes in obese rats. *BMC Res Notes* 2014;7:931.
64. Frank S, Colliver JA, Frank A. The electrocardiogram in obesity: statistical analysis of 1,029 patients. *J Am Coll Cardiol* 1986;7:295-299.
65. Dobson GP. On being the right size: heart design, mitochondrial efficiency and lifespan potential. *Clin Exp Pharmacol Physiol* 2003;30:590-597.
66. Von Döbeln W. Maximal oxygen intake, body size, and total hemoglobin in normal man. *Acta Physiol Scand* 1956;38:193-199.
67. Zong P, Zhang L, Shaban NM, et al. Left heart chamber quantification in obese patients: how does larger body size affect echocardiographic measurements? *J Am Soc Echocardiogr* 2014;27:1267-1274.
68. Hill CM, Mostafa P, Stuart AG, et al. ECG variations in patients pre- and post-local anaesthesia and analgesia. *Br Dent J* 2009;207:E23.
69. Staikou C, Stamelos M, Stavroulakis E. Impact of anaesthetic drugs and adjuvants on ECG markers of torsadogenicity. *Br J Anaesth* 2014;112:217-230.
70. Tárraga K, Spinosa H, Camacho AA. Electrocardiographic evaluation of two anesthetic combinations in dogs. *Arq Bras Med Vet Zootec* 2000;52:138-143.